Quasi-Two-Dimensional Antiferromagnetic Spin Fluctuations in the Spin-Triplet Superconductor Candidate $CeRh_2As_2$

Tong Chen,[1,*] Hasan Siddiquee,[2] Qiaozhi Xu,[2] Zack Rehfuss,[2] Shiyuan Gao,[1] Chris Lygouras,[1] Jack Drouin,[1] Vincent Morano,[1] Keenan E. Avers,[3] Christopher J. Schmitt,[4] Andrey Podlesnyak,[4] Johnpierre Paglione,[3] Sheng Ran,[2,†] Yu Song,[5,‡] and Collin Broholm[1,6,§]

[1]*Institute for Quantum Matter and Department of Physics and Astronomy, Johns Hopkins University, Baltimore, Maryland 21218, USA*
[2]*Department of Physics, Washington University in St. Louis, St. Louis, Missouri 63130, USA*
[3]*Maryland Quantum Materials Center and Department of Physics, University of Maryland, College Park, Maryland 20742, USA*
[4]*Neutron Scattering Division, Oak Ridge National Laboratory, Oak Ridge, Tennessee 37831, USA*
[5]*Center for Correlated Matter and School of Physics, Zhejiang University, Hangzhou 310058, China*
[6]*Department of Materials Science and Engineering, The Johns Hopkins University, Baltimore, Maryland 21218, USA*

(Received 5 June 2024; revised 13 November 2024; accepted 21 November 2024; published 31 December 2024)

The tetragonal heavy-fermion superconductor $CeRh_2As_2$ ($T_c = 0.3$ K) exhibits an exceptionally high critical field of 14 T for $\mathbf{B}\|\mathbf{c}$. It undergoes a field-driven first-order phase transition between superconducting states, potentially transitioning from spin-singlet to spin-triplet superconductivity. To further understand these superconducting states and the role of magnetism, we probe spin fluctuations in $CeRh_2As_2$ using neutron scattering. We find dynamic (π, π) antiferromagnetic (AFM) spin correlations with an anisotropic quasi-two-dimensional correlation volume. Our data place an upper limit of 0.31 μ_B on the staggered magnetization of corresponding Néel orders at $T = 0.08$ K. Density functional theory calculations, treating Ce $4f$ electrons as core states, show that the AFM wave vector connects significant areas of the Fermi surface. Our findings indicate that the dominant excitations in $CeRh_2As_2$ for $\hbar\omega < 1.2$ meV are magnetic and suggest that superconductivity in $CeRh_2As_2$ is mediated by AFM spin fluctuations associated with a proximate quantum critical point.

DOI: 10.1103/PhysRevLett.133.266505

While phonon-mediated superconductivity is typically incompatible with magnetism, antiferromagnetic (AFM) spin fluctuations can promote unconventional superconductivity [1,2] in various systems, including cuprates [3–6], Fe-pnictides [7–9] and chalcogenides [10,11], and heavy-fermion metals [12]. Experimental evidence for magnetically driven superconductivity includes (i) spin resonance modes in the superconducting (SC) state [13–15], and (ii) paramagnetic excitations in the normal state with energies well beyond the SC gap [16–20]. Despite extensive efforts to understand the spin dynamics of spin-singlet unconventional superconductors, research on spin-triplet superconductors has been constrained by the scarcity of model systems [15,21].

$CeRh_2As_2$ is a heavy-fermion superconductor with $T_c = 0.3$ K [22]. It adopts the tetragonal $CaBe_2Ge_2$-type structure (space group No. 129 P4/nmm), consisting of two-dimensional (2D) Ce layers stacked with As-Rh-As and Rh-As-Rh blocks along the **c** axis [Fig. 1(a) inset]. While the overall crystal structure is centrosymmetric, Ce layers are positioned between distinct blocks, leading to local inversion symmetry breaking and alternating Rashba spin-orbit coupling (SOC) [23,24]. For $\mathbf{B}\|\mathbf{c}$, $CeRh_2As_2$ exhibits pronounced anomalies in alternating current susceptibility, magnetization, and magnetostriction [22,25–30], indicating a first-order field-driven transition between different SC states [Fig. 1(a)]. Similar phase transitions within the SC state were observed in UPt_3 [31] and $CeCoIn_5$ [32] and attributed to the interplay between superconductivity and competing magnetic order parameters. In $CeRh_2As_2$, the presence of alternating Rashba SOC suggests the possibility of a transition from spin-singlet to spin-triplet superconductivity [33–42], although other scenarios may also apply [43,44].

To further understand the superconducting phases of $CeRh_2As_2$, we use neutron scattering to probe the low-temperature (T) zero-field magnetism of $CeRh_2As_2$. Our elastic scattering data reveal no significant differences between 0.08 K and 0.8 K, indicating the absence or weakness of magnetic order, and place an upper limit of 0.31 μ_B on the staggered magnetization of corresponding Néel orders at temperatures down to 0.08 K. Our inelastic magnetic neutron scattering data, however, reveal a gapless spectrum of quasi-2D AFM spin fluctuations at the

*Contact author: tchen115@jhu.edu
†Contact author: rans@wustl.edu
‡Contact author: yusong_phys@zju.edu.cn
§Contact author: broholm@jhu.edu

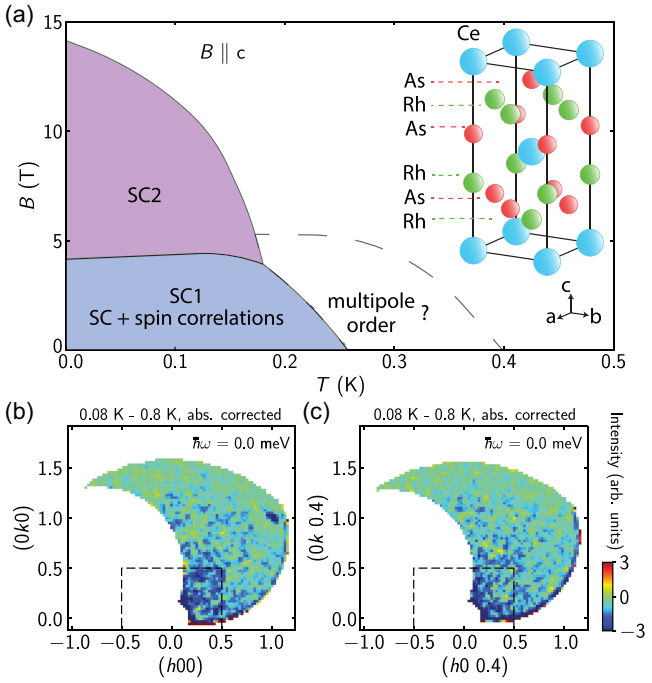

FIG. 1. (a) Schematic field-temperature phase diagram of $CeRh_2As_2$ for $\mathbf{B}\|\mathbf{c}$ based on Refs. [22,25–30]. The inset shows the crystal structure of $CeRh_2As_2$. $\mathbf{Q}$ dependence of the difference in elastic neutron scattering between $T = 0.08$ K and $T = 0.8$ K for (b) $|l| < 0.15$ and (c) $0.35 < |l| < 0.45$. Dashed lines indicate the Brillouin zone.

(π, π) wave vector $\mathbf{Q}_{\mathrm{AFM}}$ extending up to 1.2 meV. In combination with density functional theory (DFT) calculations [28,35,37,45–49] and angle-resolved photoemission spectroscopy (ARPES) measurements [46–48] that reveal Fermi-surface nesting at $\mathbf{Q}_{\mathrm{AFM}}$, our findings suggest proximity to Fermi-surface-driven magnetic criticality in $CeRh_2As_2$ [22,28], with the associated spin fluctuations playing a crucial role in the superconductivity.

$CeRh_2As_2$ single crystals were synthesized via a flux method [22,50]. The sharp resistive transition of a representative sample at $T_c = 0.3$ K is displayed in the Supplemental Material [51]. For neutron scattering experiments in the $(hk0)$ plane, ~120 crystals (0.9 g) were coaligned with a full width at half maximum (FWHM) mosaic width of 2.8 degrees for rotation around the $\mathbf{c}$ axis. As detailed in the Supplemental Material [51], precautions were taken to ensure good thermal contact between the dilution refrigerator and the sample. Neutron experiments were conducted at Oak Ridge National Laboratory using the CNCS Spectrometer [57] with a fixed incident energy E_i of 3.32 meV. Operating in the high flux mode with the disk chopper rotating at 180 Hz, this setup resulted in an FWHM elastic energy resolution of 0.17 meV.

Normalization of the measured scattering cross sections was achieved by comparing the count rate with the $\mathbf{Q}$-integrated count rate for the (110) nuclear Bragg peak.

TABLE I. Upper limits on the magnitudes of staggered magnetization in $CeRh_2As_2$ obtained from the difference between elastic neutron scattering at $T = 0.08$ K and $T = 0.8$ K shown in Figs. 1(b) and 1(c). In-plane oriented magnetic order is harder to detect due to the domain averaged polarization factor.

$\mathbf{Q}_m$	$m_{z,\max}$ (μ_B)	$m_{\|,\max}$ (μ_B)
$(\frac{1}{2}\frac{1}{2}0)$	0.10	0.14
$(\frac{1}{2}\frac{1}{2}\frac{1}{2})$	0.14	0.20
(010)	0.14	0.20
$(01\frac{1}{2})$	0.22	0.31
quasi-2D $(\frac{1}{2}\frac{1}{2})$	0.14	0.20

As detailed in the Supplemental Material [51], a scattering angle and energy transfer dependent factor was applied to background subtracted data to correct for the significant absorption cross section of $CeRh_2As_2$. When background subtraction is not feasible, uncorrected intensity data are presented in arbitrary units. In the following, momentum transfer $\mathbf{Q}$ is expressed as $\mathbf{Q} = h\mathbf{a}^* + k\mathbf{b}^* + l\mathbf{c}^*$, where (hkl) denotes Miller indices. A pair of indices (hk) specify the in-plane component of wave vector $\mathbf{Q}_\|$. Here, $a^* = b^* = 2\pi/a$ and $c^* = 2\pi/c$, with $a = b = 4.28$ Å and $c = 9.86$ Å at room temperature [22].

The difference in elastic scattering between data acquired in the SC state at 0.08 K and in the normal state at 0.8 K is shown in Figs. 1(b) and 1(c) for $l = 0$ and $l = \pm 0.4$, respectively. No diffraction peaks are apparent in either figure. These data place upper limits on magnetic ordering at specific magnetic wave vectors (see Table I and the Supplemental Material [51]).

Nuclear quadrupole resonance (NQR) [58] and nuclear magnetic resonance (NMR) [59] experiments provide evidence for an increase of the NQR and NMR linewidths in the low-field SC1 state for the As sites of As-Rh-As blocks, which has distinct Ce neighbors displaced along $\mathbf{c}$, but not for the As sites of Rh-As-Rh blocks, where Ce neighbors come in groups of four whose fields cancel out in the AFM states shown in Table I. A possible explanation is weak long- or short-range AFM ordering that is detectable with local probes such as NMR and NQR [59,60], but sufficiently weak and/or broad in $\mathbf{Q}$ to evade detection through neutron diffraction (see Table I).

Though we do not detect elastic magnetic diffraction, dynamic AFM spin correlations are apparent in the inelastic scattering. Figures 2(a)–2(d) show the $\mathbf{Q}$-dependence within the (hk) plane of the scattering intensity for various fixed $\hbar\omega$. As AFM fluctuations are observed in both paramagnetic and SC states with no discernible differences within the $\hbar\omega$ range covered, measurements taken at 0.08 K and 0.8 K are averaged and denoted as 0.4(4) K to improve statistical accuracy. The elastic data display the (110) nuclear Bragg peak from $CeRh_2As_2$, which we use for normalization and alignment. Other T-independent features in the elastic scattering are associated with the sample

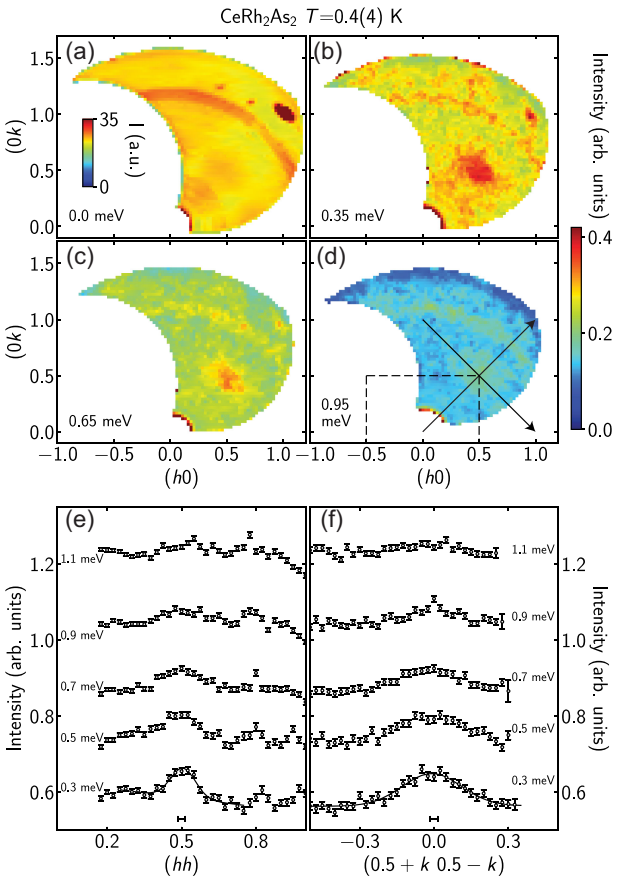

FIG. 2. (a)–(d) $\mathbf{Q}_{\parallel}$-dependence of neutron scattering from $CeRh_2As_2$ at selected $\hbar\omega$ for $T = 0.4(4)$ K and $|Q_z| < 0.5c^*$. The energy windows are 0.4 meV in (a) and 0.3 meV in (b)–(d). Arrows indicate the longitudinal (hh) and transverse $(k\bar{k})$ directions. (e),(f) Constant energy cuts along (hh) and $(k\bar{k})$ through $\mathbf{Q}_{\mathrm{AFM}} = (\frac{1}{2}\frac{1}{2})$ for selected $\hbar\omega$ with an energy window of 0.2 meV. The averaging windows are $\Delta^2\mathbf{Q} = \pm(0.15, -0.15, 0)\pm (0, 0, 0.5)$ in (e) and $\Delta^2\mathbf{Q} = \pm(0.1, 0.1, 0) \pm (0, 0, 0.5)$ in (f). Solid lines for $\hbar\omega = 0.3$ meV are Gaussian fits. The horizontal bars represent the FWHM resolution.

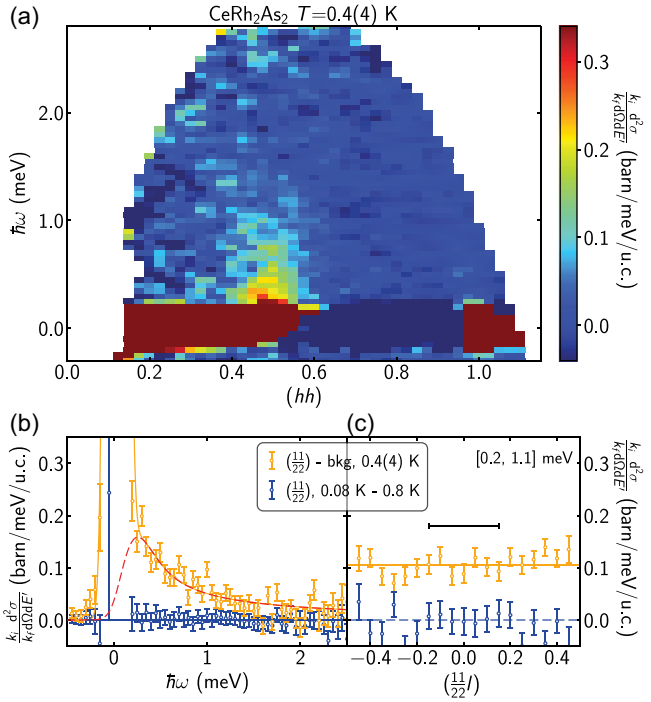

FIG. 3. (a) Background subtracted inelastic neutron scattering versus $\mathbf{Q} = (hh)$ and $\hbar\omega$ for $CeRh_2As_2$ at $T = 0.4(4)$ K. The signal averaging window is $\Delta^2\mathbf{Q} = (\pm(0.15, -0.15), \pm 0.5)$. The $|\mathbf{Q}|$ and $\hbar\omega$ dependent background was determined by averaging all data outside the signal volume. (b),(c) Background subtracted data at $T = 0.4(4)$ K in orange and the difference between $T = 0.08$ K and $T = 0.8$ K data in blue. (b) An $\hbar\omega$ scan at $\mathbf{Q}_{\mathrm{AFM}} = (\frac{1}{2}\frac{1}{2})$ averaging over $\Delta^3\mathbf{Q} = (\pm 0.1, \pm 0.1, \pm 0.5)$. The red line shows a fit to the data described in the text. (c) A scan along $\mathbf{Q} = (\frac{1}{2}\frac{1}{2}l)$ averaging over $\hbar\omega \in [0.2, 1.1]$ meV and $\Delta^2\mathbf{Q} = \pm(0.1, 0.1, 0) \pm (0.15, -0.15, 0)$. The horizontal bar represents the resolution width.

holder (powder ring and low $|\mathbf{Q}|$ diffuse scattering) and two small misaligned $CeRh_2As_2$ crystallites. At $\hbar\omega = 0.35$ meV, a diffuse peak is observed near the AFM wave vector $\mathbf{Q}_{\mathrm{AFM}} = (\frac{1}{2}\frac{1}{2})$ [Fig. 2(b)]. While the peak position persists, the intensity decreases with increasing $\hbar\omega$.

Figures 2(e) and 2(f) show constant-$\hbar\omega$ cuts through these data along the longitudinal (hh) and transverse $(k\bar{k})$ directions. These cuts show that the low-energy magnetic scattering is centered at $\mathbf{Q}_{\mathrm{AFM}}$ consistent with dynamic short-ranged AFM spin correlations as in many Ce-based heavy fermion systems including SC $CeCoIn_5$ [13]. Fitting the cuts to Gaussians, we infer dynamic correlation lengths (defined as 2/FWHM) at 0.3 meV along (hh) and $(k\bar{k})$ of $\xi_{hh} = 8.1(8)$ Å and $\xi_{k\bar{k}} = 3.4(3)$ Å, respectively. Considering the fourfold rotation axis of paramagnetic $CeRh_2As_2$, this anisotropy suggests a preferred polarization factor in the magnetic neutron scattering cross section. Specifically, scattering at $\mathbf{Q}_{\mathrm{AFM}}$ detects spin fluctuations in the plane perpendicular to $\mathbf{Q}_{\mathrm{AFM}}$, thus along $\mathbf{c}$ or $(1\bar{1}0)$, of which the latter component can give rise to the observed anisotropy. The data indicate an underlying nematic character to the AFM spin correlations, where the correlation length is longer perpendicular to than parallel to the fluctuating in-plane staggered magnetization. Such anisotropy can arise from symmetric anisotropic exchange interactions and was previously observed in iron-based superconductors [9]. Given the spin-orbital character of Ce-based magnetism, anisotropic interactions are indeed anticipated. The data specifically indicate in-plane anisotropic interactions and suggest that the fourfold rotation symmetry will be broken by the corresponding static order.

Figure 3(a) displays the $\mathbf{Q} - \omega$ dependent magnetic scattering cross section for $\mathbf{Q}\|(11)$. A ridge of low-energy excitations at $\mathbf{Q}_{\mathrm{AFM}}$ extending to 1.2 meV is apparent. Figure 3(b) shows a broad constant-$\mathbf{Q}_{\mathrm{AFM}}$ cut through these

data. While data for $|\hbar\omega| < 0.15$ meV are dominated by imperfect subtraction of the incoherent elastic scattering, we associate the tail of scattering for $\hbar\omega > 0.15$ meV that is absent on the neutron energy gain side ($\hbar\omega < -0.15$ meV) with magnetic quantum fluctuations for $k_B T \ll \hbar\omega$. To further characterize the scattering, we fit these data against a resolution-convoluted Lorentzian response function of the form

$$\mathcal{S}(\omega) = \frac{1}{1 - e^{-\beta\hbar\omega}} \frac{\chi_0 \Gamma \omega}{\Gamma^2 + \omega^2}, \tag{1}$$

plus a central Gaussian peak to account for the residual elastic background. As shown in Fig. 3(b), this model provides an excellent account of the data with a characteristic relaxation rate of $\hbar\Gamma = 0.10(4)$ meV. This suggests proximity to a quantum critical point (QCP) where $\hbar\Gamma \sim k_B T$ [13,14,61,62].

From the total magnetic scattering associated with inelastic magnetic scattering below 2.5 meV, we obtain the dynamic moment of $1.6(4)\mu_B^2$. The reduction in moment compared to the effective moment inferred from susceptibility ($\mu_{\text{eff}}^2 = 6.55\mu_B^2$ [22]) is observed in other Ce-based heavy-fermion superconductors, such as $CeCoIn_5$ [13] and $CeCu_2Si_2$ [14]. Magnetic excitations extend to much higher energies in these systems [19,20] due to crystal electric field and Kondo screening. Likewise, in $CeRh_2As_2$ we expect such interactions to define a low-energy reduced moment regime with residual AFM intersite interactions.

To probe the associated spin correlations along $\mathbf{c}$, Fig. 3(c) shows the l dependence of scattering for $\hbar\omega \in [0.2, 1.1]$ meV at $\mathbf{Q}_{\text{AFM}}$. The corresponding count rate at $\mathbf{Q}_{\text{bkg}} = (0.1, 0.7)$ where $|\mathbf{Q}_{\text{bkg}}| = |\mathbf{Q}_{\text{AFM}}|$ was used as background. The inelastic scattering at $\mathbf{Q}_{\text{AFM}}$ consistently exceeds that at $\mathbf{Q}_{\text{bkg}}$ by a nearly l-independent amount, indicating quasi-2D spin correlations. No difference between scattering at 0.08 K and 0.8 K is observed in the accessible energy range.

To gain insights into the origin of the AFM spin fluctuations in $CeRh_2As_2$, we conducted band structure calculations using DFT, treating Ce $4f$ electrons as core states. The results are shown in Fig. 4(a), with the corresponding Fermi surface displayed in Figs. 4(b)–4(d). Specifically, the Fermi surface at $l = 0$ [Fig. 4(c)] is squarelike, with sides approximately connected by $\mathbf{Q}_{\text{AFM}}$, as indicated by the red arrow. Since Ce $4f$ electrons are treated as core states, the calculated Fermi surface arises from conduction electrons that induce a Ruderman-Kittel-Kasuya-Yosida interaction between Ce $4f$ local moments, leading to AFM spin fluctuations at $\mathbf{Q}_{\text{AFM}}$. Although the strong k_z dependence of the DFT Fermi surface seems at odds with the quasi-2D character of the AFM fluctuations observed in our experiments, this discrepancy suggests the dominance of in-plane correlations, which is crucial in

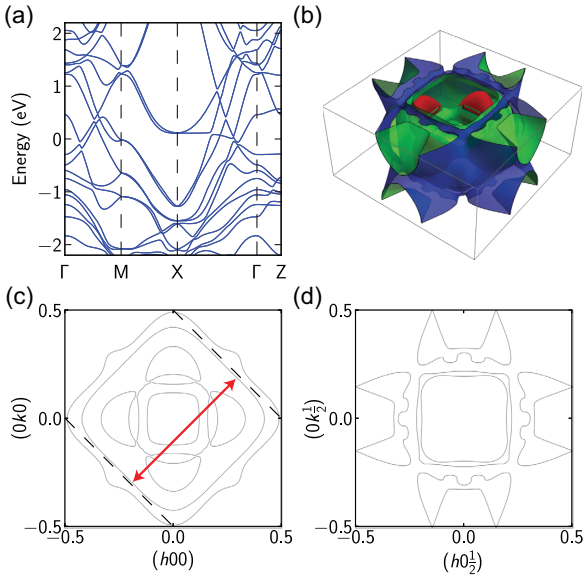

FIG. 4. (a) Electronic band structure of $CeRh_2As_2$ calculated using DFT with Ce $4f$ electrons in the core. (b)–(d) The corresponding Fermi surface as a 3D image and as 2D slices through (c) the $(hk0)$ plane and (d) the $(hk\frac{1}{2})$ plane. The red arrow indicates the wave vector $\mathbf{Q}_{\text{AFM}} = (\frac{1}{2}\frac{1}{2})$ associated with low energy inelastic magnetic neutron scattering [Fig. 3(a)], which is seen to connect significant portions of the DFT Fermi surface.

theoretical models predicting the singlet-triplet transition in $CeRh_2As_2$ [33–42]. Alternatively, as $CeRh_2As_2$ is a heavy fermion metal with $4f$ states that hybridize with the conduction bands, the spin fluctuations at $\mathbf{Q}_{\text{AFM}}$ may arise from particle-hole excitations of the heavy electron bands. The quasi-2D AFM fluctuations observed in our neutron scattering measurements uniquely identify (π, π) as the primary nesting vector, among other plausible nesting vectors suggested by recent ARPES studies [46–48].

Resistivity and specific heat measurements reveal non-Fermi-liquid behavior at low T, which indicates proximity to a QCP [22,28]. Our observations of anisotropic AFM fluctuations in $CeRh_2As_2$ suggest that this QCP has a nematic 2D AFM character, where the proximate ordered phase likely breaks the fourfold rotational symmetry of the underlying crystal lattice. Quantum critical fluctuations near a QCP are natural candidates as bosonic modes that drive superconductivity. Accordingly, our findings highlight the prominent role of AFM spin fluctuations in the superconductivity of $CeRh_2As_2$, as in many other heavy-fermion superconductors. The momentum and energy dependence of the spin fluctuations in $CeRh_2As_2$ revealed in our work provide stringent constraints on models of its zero-field superconductivity.

Time reversal and inversion symmetry in a metal enable even parity spin-singlet superconductivity and odd parity spin-triplet superconductivity, respectively. However, in superconductors lacking global inversion symmetry,

electronic antisymmetric SOC, such as Rashba SOC, lift the spin degeneracy and mix spin-singlet and spin-triplet states [63,64]. The unique local inversion symmetry breaking of $CeRh_2As_2$ naturally connects it to the previous proposal of noncentrosymmetric superconductivity in $CeCoIn_5$ multilayers [32]. Alternating Rashba SOC has been known to support distinct SC phases with spin-singlet and spin-triplet symmetries in the field-temperature phase diagram [24,63]. Experimental results in $CeRh_2As_2$ appear consistent with this picture, suggesting that the SC1 and high-field SC2 phases correspond to spin-singlet and spin-triplet pairing states, respectively. However, the recent NMR study [59] reported T-dependent Knight shifts, suggesting spin-singlet pairing in both SC phases, adding complexity to the Rashba SOC scenario. Since AFM spin fluctuations are typically seen in spin-singlet unconventional superconductors and ferromagnetic spin fluctuations are expected for spin-triplet superconductors, our observation of AFM spin fluctuations at zero field is consistent with spin-singlet pairing in the SC1 phase. The fact that these AFM fluctuations extend to 1.2 meV $\gg k_B T_C$ suggests they will persist in the field-induced SC2 phase. In such a scenario, the SC2 phase should exhibit a prominent spin-singlet pairing component, consistent with the NMR measurement [59]. However, as research on UTe_2 revealed, AFM spin fluctuations can mediate spin-triplet superconductivity [15]. Thus, additional theoretical and experimental efforts are necessary to elucidate the symmetry and mechanism of the SC2 phase. Nevertheless, our observation of AFM spin fluctuations places strong constraints on models of its field-induced superconductor-superconductor transition.

We have investigated the magnetic excitations in $CeRh_2As_2$ using neutron scattering, revealing nematic quasi-2D AFM spin fluctuations centered at $\mathbf{Q}_{AFM}$ and extending up to 1.2 meV at low T. Our neutron scattering measurements and DFT calculations indicate $\mathbf{Q}_{AFM}$ fluctuations result from the nesting of heavy quasi-2D Ce $4f$ electrons, which are also responsible for the heavy-fermion superconductivity in $CeRh_2As_2$. These findings indicate a crucial role of AFM spin fluctuations in the superconductivity of $CeRh_2As_2$, although the connection to the field-induced superconductor-superconductor transition remains to be understood.

Acknowledgments—We gratefully acknowledge the support from T. Xie and R. Kumar during the experiments and the valuable discussions with S.-H. Baek, P. Dai, Y. Liu, E. Hassinger, and D. Agterberg. Work at the Institute for Quantum Matter, was supported by DOE, Office of Science, Basic Energy Sciences under Award No. DE-SC0019331 and No. DE-SC0024469. Research at Washington University was supported by the National Science Foundation (NSF) Division of Materials Research Award No. DMR-2236528. Research at the University of Maryland was supported by the U.S. Department of Energy (DOE) Award No. DE-SC-0019154 (experimental preparation). J. P. acknowledges support from the Gordon and Betty Moore Foundation's EPiQS Initiative through Grant No. GBMF4419. C. B. was supported by the Gordon and Betty Moore Foundation EPIQS program under GBMF9456 and acknowledges the hospitality of the Instituto de Física at UNAM, México. Research at Zhejiang University was supported by the National Key R&D Program of China (No. 2022YFA1402200). A portion of this research used resources at the Spallation Neutron Source, a DOE Office of Science User Facility operated by ORNL.

[1] T. Moriya and K. Ueda, Spin fluctuations and high temperature superconductivity, Adv. Phys. **49**, 555 (2000).
[2] D. J. Scalapino, A common thread: The pairing interaction for unconventional superconductors, Rev. Mod. Phys. **84**, 1383 (2012).
[3] J. Rossat-Mignod, L. Regnault, C. Vettier, P. Bourges, P. Burlet, J. Bossy, J. Henry, and G. Lapertot, Neutron scattering study of the $YBa_2Cu_3O_{6+x}$ system, Physica (Amsterdam) **185C**, 86 (1991).
[4] H. A. Mook, M. Yethiraj, G. Aeppli, T. E. Mason, and T. Armstrong, Polarized neutron determination of the magnetic excitations in $YBa_2Cu_3O_7$, Phys. Rev. Lett. **70**, 3490 (1993).
[5] H. F. Fong, B. Keimer, P. W. Anderson, D. Reznik, F. Doğan, and I. A. Aksay, Phonon and magnetic neutron scattering at 41 meV in $YBa_2Cu_3O_7$, Phys. Rev. Lett. **75**, 316 (1995).
[6] J. M. Tranquada, G. Xu, and I. A. Zaliznyak, Superconductivity, antiferromagnetism, and neutron scattering, J. Magn. Magn. Mater. **350**, 148 (2014).
[7] A. Christianson, E. Goremychkin, R. Osborn, S. Rosenkranz, M. Lumsden, C. Malliakas, I. Todorov, H. Claus, D. Chung, M. Kanatzidis *et al.*, Unconventional superconductivity in $Ba_{0.6}K_{0.4}Fe_2As_2$ from inelastic neutron scattering, Nature (London) **456**, 930 (2008).
[8] D. Inosov, J. Park, P. Bourges, D. Sun, Y. Sidis, A. Schneidewind, K. Hradil, D. Haug, C. Lin, B. Keimer *et al.*, Normal-state spin dynamics and temperature-dependent spin-resonance energy in optimally doped $BaFe_{1.85}Co_{0.15}As_2$, Nat. Phys. **6**, 178 (2010).
[9] P. Dai, Antiferromagnetic order and spin dynamics in iron-based superconductors, Rev. Mod. Phys. **87**, 855 (2015).
[10] Q. Wang, Y. Shen, B. Pan, Y. Hao, M. Ma, F. Zhou, P. Steffens, K. Schmalzl, T. Forrest, M. Abdel-Hafiez *et al.*, Strong interplay between stripe spin fluctuations, nematicity and superconductivity in FeSe, Nat. Mater. **15**, 159 (2016).
[11] T. Chen, Y. Chen, A. Kreisel, X. Lu, A. Schneidewind, Y. Qiu, J. Park, T. G. Perring, J. R. Stewart, H. Cao *et al.*, Anisotropic spin fluctuations in detwinned FeSe, Nat. Mater. **18**, 709 (2019).
[12] M. Smidman, O. Stockert, E. M. Nica, Y. Liu, H. Yuan, Q. Si, and F. Steglich, Colloquium: Unconventional fully gapped superconductivity in the heavy-fermion metal $CeCu_2Si_2$, Rev. Mod. Phys. **95**, 031002 (2023).

[13] C. Stock, C. Broholm, J. Hudis, H. J. Kang, and C. Petrovic, Spin resonance in the d-wave superconductor $CeCoIn_5$, Phys. Rev. Lett. **100**, 087001 (2008).

[14] O. Stockert, J. Arndt, E. Faulhaber, C. Geibel, H. S. Jeevan, S. Kirchner, M. Loewenhaupt, K. Schmalzl, W. Schmidt, Q. Si *et al.*, Magnetically driven superconductivity in $CeCu_2Si_2$, Nat. Phys. **7**, 119 (2011).

[15] C. Duan, R. Baumbach, A. Podlesnyak, Y. Deng, C. Moir, A. J. Breindel, M. B. Maple, E. Nica, Q. Si, and P. Dai, Resonance from antiferromagnetic spin fluctuations for superconductivity in UTe_2, Nature (London) **600**, 636 (2021).

[16] L. P. Regnault, W. A. C. Erkelens, J. Rossat-Mignod, P. Lejay, and J. Flouquet, Neutron scattering study of the heavy-fermion compound $CeRu_2Si_2$, Phys. Rev. B **38**, 4481 (1988).

[17] J. Arndt, O. Stockert, K. Schmalzl, E. Faulhaber, H. S. Jeevan, C. Geibel, W. Schmidt, M. Loewenhaupt, and F. Steglich, Spin fluctuations in normal state $CeCu_2Si_2$ on approaching the quantum critical point, Phys. Rev. Lett. **106**, 246401 (2011).

[18] Q. Wang, Y. Shen, B. Pan, X. Zhang, K. Ikeuchi, K. Iida, A. Christianson, H. Walker, D. Adroja, M. Abdel-Hafiez *et al.*, Magnetic ground state of FeSe, Nat. Commun. **7**, 12182 (2016).

[19] Y. Song, W. Wang, J. S. Van Dyke, N. Pouse, S. Ran, D. Yazici, A. Schneidewind, P. Čermák, Y. Qiu, M. Maple *et al.*, Nature of the spin resonance mode in $CeCoIn_5$, Commun. Phys. **3**, 98 (2020).

[20] Y. Song, W. Wang, C. Cao, Z. Yamani, Y. Xu, Y. Sheng, W. Löser, Y. Qiu, Y.-f. Yang, R. J. Birgeneau *et al.*, High-energy magnetic excitations from heavy quasiparticles in $CeRu_2Si_2$, npj Quantum Mater. **6**, 60 (2021).

[21] S. Carr, Diverse neutron scattering measurements in unconventional superconductors, Ph.D. thesis, Rice Research Repository (R-3), Houston, TX, 2016.

[22] S. Khim, J. Landaeta, J. Banda, N. Bannor, M. Brando, P. Brydon, D. Hafner, R. Küchler, R. Cardoso-Gil, U. Stockert *et al.*, Field-induced transition within the superconducting state of $CeRh_2As_2$, Science **373**, 1012 (2021).

[23] G. Bihlmayer, P. Noël, D. V. Vyalikh, E. V. Chulkov, and A. Manchon, Rashba-like physics in condensed matter, Nat. Rev. Phys. **4**, 642 (2022).

[24] M. H. Fischer, M. Sigrist, D. F. Agterberg, and Y. Yanase, Superconductivity and local inversion-symmetry breaking, Annu. Rev. Condens. Matter Phys. **14**, 153 (2023).

[25] J. Landaeta, P. Khanenko, D. Cavanagh, C. Geibel, S. Khim, S. Mishra, I. Sheikin, P. Brydon, D. Agterberg, M. Brando *et al.*, Field-angle dependence reveals odd-parity superconductivity in $CeRh_2As_2$, Phys. Rev. X **12**, 031001 (2022).

[26] S. Mishra, Y. Liu, E. D. Bauer, F. Ronning, and S. M. Thomas, Anisotropic magnetotransport properties of the heavy-fermion superconductor $CeRh_2As_2$, Phys. Rev. B **106**, L140502 (2022).

[27] S. Onishi, U. Stockert, S. Khim, J. Banda, M. Brando, and E. Hassinger, Low-temperature thermal conductivity of the two-phase superconductor $CeRh_2As_2$, Front. Electron. Mater. **2**, 880579 (2022).

[28] D. Hafner, P. Khanenko, E.-O. Eljaouhari, R. Küchler, J. Banda, N. Bannor, T. Lühmann, J. Landaeta, S. Mishra, I. Sheikin *et al.*, Possible quadrupole density wave in the superconducting Kondo lattice $CeRh_2As_2$, Phys. Rev. X **12**, 011023 (2022).

[29] K. Semeniuk, D. Hafner, P. Khanenko, T. Lühmann, J. Banda, J. Landaeta, C. Geibel, S. Khim, E. Hassinger, and M. Brando, Decoupling multiphase superconductivity from normal state ordering in $CeRh_2As_2$, Phys. Rev. B **107**, L220504 (2023).

[30] G. Chajewski and D. Kaczorowski, Discovery of magnetic phase transitions in heavy-fermion superconductor $CeRh_2As_2$, Phys. Rev. Lett. **132**, 076504 (2024).

[31] G. Aeppli, D. Bishop, C. Broholm, E. Bucher, K. Siemensmeyer, M. Steiner, and N. Stüsser, Magnetic order in the different superconducting states of UPt_3, Phys. Rev. Lett. **63**, 676 (1989).

[32] T. Yoshida, M. Sigrist, and Y. Yanase, Pair-density wave states through spin-orbit coupling in multilayer superconductors, Phys. Rev. B **86**, 134514 (2012).

[33] E. G. Schertenleib, M. H. Fischer, and M. Sigrist, Unusual H-T phase diagram of $CeRh_2As_2$: The role of staggered noncentrosymmetricity, Phys. Rev. Res. **3**, 023179 (2021).

[34] A. Skurativska, M. Sigrist, and M. H. Fischer, Spin response and topology of a staggered-Rashba superconductor, Phys. Rev. Res. **3**, 033133 (2021).

[35] K. Nogaki, A. Daido, J. Ishizuka, and Y. Yanase, Topological crystalline superconductivity in locally noncentrosymmetric $CeRh_2As_2$, Phys. Rev. Res. **3**, L032071 (2021).

[36] D. Möckli and A. Ramires, Superconductivity in disordered locally noncentrosymmetric materials: An application to $CeRh_2As_2$, Phys. Rev. B **104**, 134517 (2021).

[37] D. C. Cavanagh, T. Shishidou, M. Weinert, P. M. R. Brydon, and D. F. Agterberg, Nonsymmorphic symmetry and field-driven odd-parity pairing in $CeRh_2As_2$, Phys. Rev. B **105**, L020505 (2022).

[38] K. Nogaki and Y. Yanase, Even-odd parity transition in strongly correlated locally noncentrosymmetric superconductors: Application to $CeRh_2As_2$, Phys. Rev. B **106**, L100504 (2022).

[39] D. C. Cavanagh, D. F. Agterberg, and P. M. R. Brydon, Pair breaking in superconductors with strong spin-orbit coupling, Phys. Rev. B **107**, L060504 (2023).

[40] Y. Yanase, A. Daido, K. Takasan, and T. Yoshida, Topological d-wave superconductivity in two dimensions, Physica (Amsterdam) **140E**, 115143 (2022).

[41] H. G. Suh, Y. Yu, T. Shishidou, M. Weinert, P. M. R. Brydon, and D. F. Agterberg, Superconductivity of anomalous pseudospin in nonsymmorphic materials, Phys. Rev. Res. **5**, 033204 (2023).

[42] A. L. Szabó, M. H. Fischer, and M. Sigrist, Effects of nucleation at a first-order transition between two superconducting phases: Application to $CeRh_2As_2$, Phys. Rev. Res. **6**, 023080 (2024).

[43] K. Machida, Violation of Pauli-clogston limit in the heavy-fermion superconductor $CeRh_2As_2$: Duality of itinerant and localized $4f$ electrons, Phys. Rev. B **106**, 184509 (2022).

[44] T. Hazra and P. Coleman, Triplet pairing mechanisms from Hund's-Kondo models: Applications to UTe_2 and $CeRh_2As_2$, Phys. Rev. Lett. **130**, 136002 (2023).

[45] A. Ptok, K. J. Kapcia, P. T. Jochym, J. Łażewski, A. M. Oleś, and P. Piekarz, Electronic and dynamical properties of $CeRh_2As_2$: Role of Rh_2As_2 layers and expected orbital order, Phys. Rev. B **104**, L041109 (2021).

[46] Y. Wu, Y. Zhang, S. Ju, Y. Hu, Y. Huang, Y. Zhang, H. Zhang, H. Zheng, G. Yang, E.-O. Eljaouhari *et al.*, Fermi surface nesting with heavy quasiparticles in the locally noncentrosymmetric superconductor $CeRh_2As_2$, Chin. Phys. Lett. **41**, 097403 (2024).

[47] X. Chen, L. Wang, J. Ishizuka, R. Zhang, K. Nogaki, Y. Cheng, F. Yang, Z. Chen, F. Zhu, Z. Liu *et al.*, Coexistence of near-E_F flat band and van Hove singularity in a two-phase superconductor, Phys. Rev. X **14**, 021048 (2024).

[48] B. Chen, H. Liu, Q.-Y. Wu, C. Zhang, X.-Q. Ye, Y.-Z. Zhao, J.-J. Song, X.-Y. Tian, B.-L. Tan, Z.-T. Liu *et al.*, Exploring possible Fermi surface nesting and the nature of heavy quasiparticles in the spin-triplet superconductor candidate $CeRh_2As_2$, Phys. Rev. B **110**, L041120 (2024).

[49] J. Ishizuka, K. Nogaki, M. Sigrist, and Y. Yanase, Correlation-induced Fermi surface evolution and topological crystalline superconductivity in $CeRh_2As_2$, Phys. Rev. B **110**, L140505 (2024).

[50] H. Siddiquee, Z. Rehfuss, C. Broyles, and S. Ran, Pressure dependence of superconductivity in $CeRh_2As_2$, Phys. Rev. B **108**, L020504 (2023).

[51] See Supplemental Material at http://link.aps.org/supplemental/10.1103/PhysRevLett.133.266505 which includes Refs. [52–56] for sample characterization, data normalization, and nesting function calculation.

[52] T. Hahn, U. Shmueli, and J. W. Arthur, *International Tables for Crystallography* (Reidel, Dordrecht, 1983), Vol. 1.

[53] O. Arnold, J.-C. Bilheux, J. Borreguero, A. Buts, S. I. Campbell, L. Chapon, M. Doucet, N. Draper, R. F. Leal, M. Gigg *et al.*, Mantid–data analysis and visualization package for neutron scattering and μSR experiments, Nucl. Instrum. Methods Phys. Res., Sect. **764**, 156 (2014).

[54] C. Dwiggins, Rapid calculation of x-ray absorption correction factors for cylinders to an accuracy of 0.1%, Acta Crystallogr. Sect. A **31**, 146 (1975).

[55] NIST center for neutron research tabulated neutron scattering lengths and cross sections, https://www.ncnr.nist.gov/resources/n-lengths/list.html.

[56] V. F. Sears, Neutron scattering lengths and cross sections, Neutron News **3**, 26 (1992).

[57] G. Ehlers, A. A. Podlesnyak, J. L. Niedziela, E. B. Iverson, and P. E. Sokol, The new cold neutron chopper spectrometer at the spallation neutron source: Design and performance, Rev. Sci. Instrum. **82**, 085108 (2011).

[58] M. Kibune, S. Kitagawa, K. Kinjo, S. Ogata, M. Manago, T. Taniguchi, K. Ishida, M. Brando, E. Hassinger, H. Rosner *et al.*, Observation of antiferromagnetic order as odd-parity multipoles inside the superconducting phase in $CeRh_2As_2$, Phys. Rev. Lett. **128**, 057002 (2022).

[59] S. Ogata, S. Kitagawa, K. Kinjo, K. Ishida, M. Brando, E. Hassinger, C. Geibel, and S. Khim, Parity transition of spin-singlet superconductivity using sublattice degrees of freedom, Phys. Rev. Lett. **130**, 166001 (2023).

[60] S. Kitagawa, M. Kibune, K. Kinjo, M. Manago, T. Taniguchi, K. Ishida, M. Brando, E. Hassinger, C. Geibel, and S. Khim, Two-dimensional XY-type magnetic properties of locally noncentrosymmetric superconductor $CeRh_2As_2$, J. Phys. Soc. Jpn. **91**, 043702 (2022).

[61] C. Broholm, J. K. Kjems, G. Aeppli, Z. Fisk, J. L. Smith, S. M. Shapiro, G. Shirane, and H. R. Ott, Spin fluctuations in the antiferromagnetic heavy-fermion system U_2Zn_{17}, Phys. Rev. Lett. **58**, 917 (1987).

[62] O. Stockert, E. Faulhaber, K. Schmalzl, W. Schmidt, H. Jeevan, M. Deppe, C. Geibel, T. Cichorek, T. Nakanishi, M. Loewenhaupt *et al.*, Peculiarities of the antiferromagnetism in $CeCu_2Si_2$, J. Phys. Conf. Ser. **51**, 211 (2006).

[63] E. M. Nica, S. Ran, L. Jiao, and Q. Si, Multiple superconducting phases in heavy-fermion metals, Front. Electron. Mater. **2**, 944873 (2022).

[64] L. P. Gor'kov and E. I. Rashba, Superconducting 2D system with lifted spin degeneracy: Mixed singlet-triplet state, Phys. Rev. Lett. **87**, 037004 (2001).